Reaction dynamics of $C(^1D)+H_2(v)\rightarrow CH(X\,^2\Pi)+H$

Klaus Mikulecky and Karl-Heinz Gericke
Institut für Physikalische und Theoretische Chemie der Johann Wolfgang Goethe-Universität, Niederurseler Hang, D-6000 Frankfurt am Main 50, Germany

(Received 4 August 1992; accepted 7 October 1992)

The $CH(X\,^2\Pi,v,J,\Omega,\Lambda)$ product state distribution from the reaction $C(^1D)+H_2(v)\rightarrow CH+H$ was determined by laser-induced fluorescence (LIF) where the $B\,^2\Sigma$–$X\,^2\Pi$ transitions were probed. Most of the available energy is released as translation. A nearly thermal rotational distribution is obtained for $CH(v=0,1)$. Only a small fraction, 4.1×10^{-4}, of the CH products is formed in the vibrationally excited state. A higher propensity for the production of CH in the symmetric $\Pi(A')$ Λ sublevels is evident. For studying the influence of vibrational excitation on the reaction dynamics, H_2 was excited to its first vibrational state via stimulated Raman pumping (SRP). $H_2(v=1)$ increases the reaction rate and enhances the population of higher rotational states, but diminishes the Λ selectivity. The vibrational population ratio $P(v=0)/P(v=1)$ of the CH product remains unaltered. Insertion of the $C(^1D)$ atom into the H_2 bond is the major reaction mechanism, but the probability for an abstractive process seems to increase when $H_2(v=1)$ is reacting with $C(^1D)$.

INTRODUCTION

The dynamics of elementary reactions involving a vibrationally excited reactant are a topic scarcely investigated yet. This is due to the difficulties arising from the necessity to excite a rotational–vibrational state selectively in order to perform a state-to-state experiment. This has become possible only recently with the availability of narrow bandwidth high power lasers which are able to excite rotational–vibrational transitions in the infrared region. As an example, the reaction of hydrogen atoms with vibrationally excited water molecules may be quoted here.[1]

We used a different way of excitation, stimulated Raman pumping (SRP), a well understood method used successfully in the past.[2–5] Apart from stimulated emission pumping (SEP) there is no other way of selective excitation than SRP, for H_2 does not exhibit an ir spectrum. The only reaction dynamics with vibrationally excited H_2 investigated to date concern the processes[4(a),4(b),5]

$$H+H_2(v)\rightarrow HD+H \tag{1}$$

and

$$O(^1D)+H_2(v=1)\rightarrow OH+H. \tag{2}$$

Now we would like to present measurements on a reaction closely related to reaction (2), the reaction of electronically excited carbon atoms with molecular hydrogen

$$C(^1D)+H_2(v)\rightarrow CH(X\,^2\Pi,v,J)+H. \tag{3}$$

Both reactions have the existence of a stable intermediate in common (H_2O, respectively, CH_2). So far there have been investigations concerning the kinetics[6–8] and dynamics of this reaction and its isotopic variant involving H_2 in its vibrational ground state,[9–11] including the determination of the rotational and electronic fine structure product state distribution. The reaction rate of reaction (3), which is exothermic by 24.8 kJ mol^{-1}, has been reported differently in literature, values of 4.1×10^{-11} (Ref. 6) and 2.6×10^{-10} cm^3 molecule^{-1} s^{-1} (Ref. 7) are published. There is no comment on the difference of a factor of 6.

The dynamical measurements revealed a statistically controlled partition of energy into the rotational states of the CH product in the lowest vibrational state, $v''=0$. Vibrationally excited CH was not observed. The rotational state distribution yields a rotational temperature of about 1600 K for the $\Pi(A'')$ and 2100 K for the $\Pi(A')$ component.[11] A determination of the Λ-substate population distribution has been performed by Jursich and Wiesenfeld.[10] They found a slightly higher population in the $\Pi(A')$ substate. The ratio $\Pi(A')/\Pi(A'')$ is approximately 1.4 ± 0.2 in the high J limit.

There have not been many attempts for theoretical calculations on reaction (3), but there are calculations of the $CH_2(\tilde{a}\,^1A_1)$ potential energy surface. $CH_2(\tilde{a}\,^1A_1)$ is important as transition state in reaction (3).[12–14] To our knowledge, just one trajectory calculation has been performed.[12] The potential energy surface was constructed by the VB/DIM method.[12] The trajectory calculation dealt with the question whether reaction (3) occurs via an insertion or an abstraction path, a question which has been discussed for the related reaction (2) in the last few years also. In order to determine the influence of translationally excited reactants, the collision energies were varied from 1/32 to 16 eV. Unfortunately, there are no calculations for the case of vibrationally excited H_2, as were performed for the $O(^1D)$ reaction.[15,16]

In the case of an insertion process, where C_{2v} symmetry is maintained, the trajectories run on the $CH_2(\tilde{a}\,^1A_1)$ surface, which does not exhibit any barrier to the reaction. The collision complex in $C_{\infty v}$ symmetry, on the other hand, which occurs during an abstraction reaction, shows a barrier of 40.5 kJ mol^{-1} (Ref. 12) or 62.7 kJ mol^{-1}.[13] The trajectory calculations result in a 99% probability for the insertion process.[12] These features of the potential energy surfaces are quite similar to the properties of the $H_2O(\tilde{X}\,^1A_1)$ surface, which is involved in the reaction of

 0021-9606/93/021244-8$06.00

$O(^1D)$ with H_2. References on the $H_2O(\tilde{X}\,^1A_1)$ calculations may be found in Ref. 5.

We chose reaction (3) for our investigation because of its weak exothermicity and the close relation to reaction (2). The exothermicity of the reaction is only 2040 cm^{-1}, so there are large effects to be expected, because vibrationally excited H_2 transfers an additional amount of energy of 4155 cm^{-1} to the collision complex. This should be compared with the $O(^1D)+H_2$ reaction where the exothermicity is 15 180 cm^{-1}, and vibrational excitation of H_2 causes detectable effects on the reaction dynamics.

For our measurements we excited the B–X transition of CH. Compared to A–X the B–X transition can be resolved better, because the A–X is a $^2\Delta$–$^2\Pi$ transition which shows more spectral lines and might exhibit too many overlapping transitions to be resolved by our devices. For probing the C–X transition we would have to use frequency doubling of the dye laser, which decreases the probe power drastically. Apart from this, its fluorescence lifetime is about 10 ns which makes detection a problem.

EXPERIMENT

Carbon atoms in their electronically excited ^1D state were prepared by the pulsed laser photolysis of carbon suboxide at 157 nm. The 157 nm photolysis yields a mixture of 3% $C(^1D)$ and 97% $C(^3P)$[17] from the excitation of the absorption band centered at 158 nm with an absorption cross section of 2.6×10^{-16} cm^2.[18] Carbon suboxide was prepared by dehydration of malonic acid with subsequent distillation[19] and vaporized prior to the experiments into a 6 ℓ glass flask at a pressure below 100 Torr to reduce polymerization. When not used for the experiment, C_3O_2 was stored under liquid nitrogen. The reactants were mixed in the vacuum chamber under flow conditions by establishing a stable H_2 pressure and adding C_3O_2 afterwards.

The reaction chamber was evacuated with an oil diffusion pump to a base pressure below 10^{-2} Pa. The partial pressures for C_3O_2 and H_2 were 0.8 and 14 Pa, respectively, controlled by a MKS Baratron capacitance gauge. The reactants entered through stainless steel pipes and valves. The reaction was initiated by firing the 157 nm F_2 laser (Lambda-Physik EMG 201 MSC), whose strongly divergent beam was focused by a MgF_2 lens ($f=10$ cm) into the cell. This laser emitted pulses of 3 mJ with a duration of 15 ns. Due to absorption of the 157 nm light in air the beam path had to be flushed with nitrogen.

In order to reduce the strong C_3O_2 absorption of the photolysis wavelength at 157 nm along the beam path, we introduced H_2 through the same port of the vacuum chamber where the photolysis beam entered also. Towards the reaction area the gas flow had to pass a 5 mm orifice to avoid backstreaming of C_3O_2. This resulted in an increased signal intensity and prolonged cleaning intervals for the MgF_2 lens, on which solid carbon was deposited.

The CH product was probed by LIF with an excimer-laser pumped dye laser (Lambda Physik LPX 100 and FL 2002E) at a delay of 360 ns after initiation. The dye laser was operated with a mixture of PBBO and QUI at wavelengths between 385 and 406 nm with pulse energies of about 4 mJ and a bandwidth of 0.3 cm^{-1} (FWHM). This wavelength range covers the ($B\,^2\Sigma^-\leftarrow X\,^2\Pi$) transition of CH. The (0–0) vibrational band starts at 387.4 nm, the (1–1) band at 402.5 nm. The focused probe laser beam intersected the photolysis beam rectangularly. Predissociation of the $B\,^2\Sigma^-$ state of CH did not cause any problems because it starts from rotational–vibrational levels above $N'=17$ in $v'=0$ and $N'=8$ in $v'=1$ (Ref. 20) which correspond to unpopulated rotational–vibrational states in the $X\,^2\Pi$ ground state.

The output power of the dye laser was monitored by a photoelectric detector (Hamamatsu). The LIF signal was detected by a photomultiplier (Valvo) through focusing optics and an interference filter with a transmission range of (391 ± 10) nm. The LIF intensities were corrected for influences of the filter.

Experiments with vibrationally excited hydrogen were performed by focusing the frequency doubled output of a Nd:YAG laser (Spectron SL2Q) through a H_2 pressure Raman shifter into the reaction chamber. The YAG laser was triggered 50 ns prior to the photolysis laser and counterpropagated the probe laser beam collinearly. Both beams were focused into the detection area of the multiplier optics in the center of the vacuum chamber where they intersected the photolysis laser beam. The Raman shifter generated several orders of both the Stokes and the anti-Stokes radiation of hydrogen, which are able to excite the ($v=1\leftarrow v=0$) vibrational transition of H_2 in the vacuum chamber.[1–3] An estimated portion of 20% of the $H_2(v=0)$ can be excited this way.[4] There is no vibrational relaxation of H_2 possible, for the radiative deactivation is dipole forbidden and the number of collisions is too low. We were able to observe a CH LIF signal even when there was only the Raman shifter operating, i.e., when there was no photolysis radiation. This was likely to be the outcome of a two photon excitation of C_3O_2 which was reached at a wavelength of 320 nm, the third anti-Stokes order of the Raman shifter. We decided to cut off this wavelength by a glass plate in order to have better defined conditions for the photolysis, but used this effect to align the overlap of the H_2 excitation and CH probe beams. Thus use of the Raman shifter does not cause any CH LIF signal.

The repetition rate of 10 Hz and the delay times were controlled by a digital delay generator (Stanford). For measurements with vibrationally excited H_2 we used a trigger suspender for the Q switch of the Nd:YAG laser. This device divided the main trigger frequency by two so that every second pulse triggered the Q switch. This way, only at every second pulse $C(^1D)$ reacted with vibrationally excited H_2. This allowed us to perform precise differential measurements on the influence of the vibrational excitation within a single scan.

RESULTS

The lines of the CH ($B\,^2\Sigma^-,v'\leftarrow X\,^2\Pi,v''$) transition were assigned following the tables in Refs. 21 and 22, using additional information from Refs. 20 and 23. Normalization of the line intensities with respect to their transition

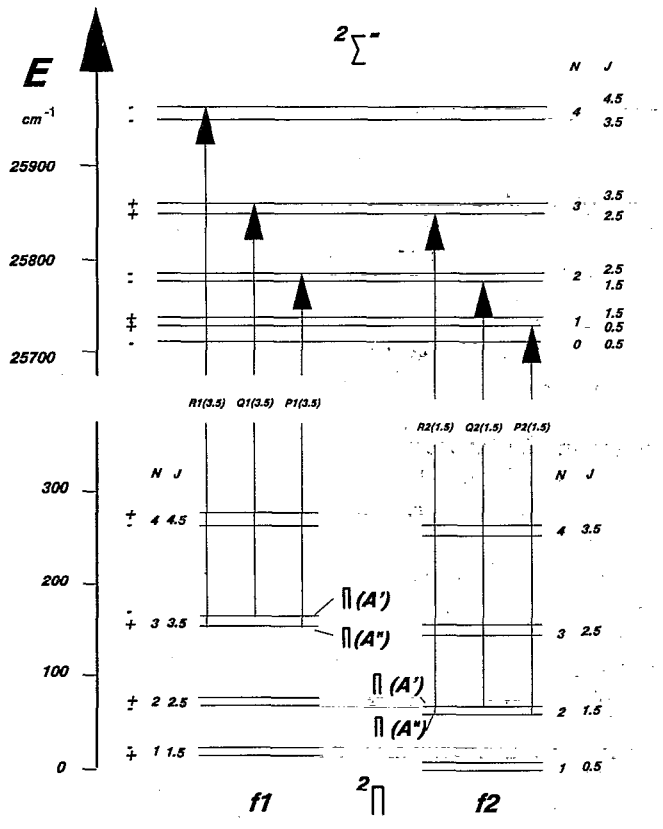

FIG. 1. Term scheme of the $X\,^2\Pi$ and $B\,^2\Sigma^-$ states. The transitions are indicated by arrows.

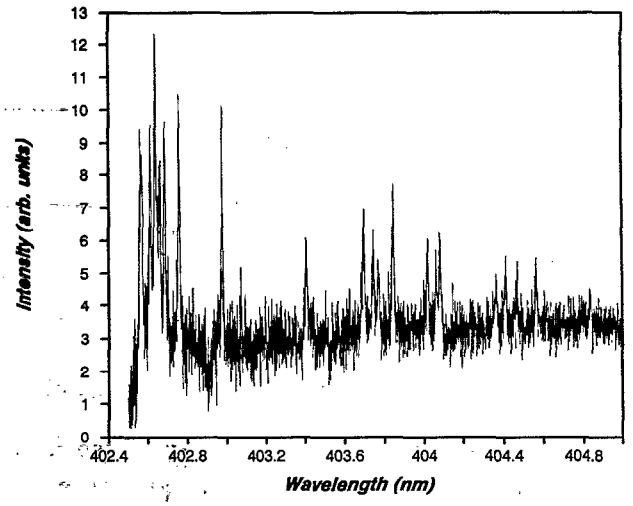

FIG. 2. Portion of the CH $[B\,^2\Sigma^-(v=1)\leftarrow X\,^2\Pi(v=1)]$ LIF spectrum in the reaction $C(^1D)+H_2\rightarrow CH+H$.

probabilities was not necessary, because we worked with a spectral power density of about 4 MW/($cm^2\,cm^{-1}$) well above the saturation level.[24(a)] Figure 1 shows the transitions in the B–X system of CH.

Vibrational distribution

We report the first observation of $CH(X\,^2\Pi,\ v''=1)$ from reaction (3). $CH(v''=1)$ is monitored with a sufficient S/N ratio at about 1.3 Pa C_3O_2 and 22 Pa H_2 partial pressures. The $CH(v''=1)$ LIF spectrum is shown in Fig. 2.

The lines were observable up to $N''=6$, so the predissociation limit of $N'=8$ in the B state was not reached. The population ratio $P(v''=1)/P(v''=0)$ has been determined by integration over the line intensities of the P_1 branch in $v''=0$ and the R_1 branch in $v''=1$ up to the highest observable rotational states. Missing or blended lines were interpolated. Scale differences were ruled out with a combining scan for the P_1 (14.5) and the (1–1) band head. So a value of $P(v''=1)/P(v''=0)=(3.9\pm2)\times10^{-4}$ was obtained. This number is subject to a correction coming from the Einstein A coefficients for the transitions ($B\,^2\Sigma^-v=1\rightarrow X\,^2\Pi\ v=1$) and ($B\,^2\Sigma^-v=1\rightarrow X\,^2\Pi\ v=0$). The laser induced fluorescence from the B state in $v'=1$ is expected to be divided into the $(1\rightarrow1)$ channel, which we observed, and into the $(1\rightarrow0)$ channel below 370 nm. The radiation of the latter is rejected by the interference filter attached to the photomultiplier optics, so part of the fluorescence light is not detected. From the Franck–Condon factors for the (1–1) and (1–0) transitions[25] we calculated a fluorescence branching ratio of 82% to (1–1) and 18% to (1–0). Analogously, we obtained for the competing fluorescence paths (0–0) and (0–1) a branching of 88% to (0–0) and 12% to (0–1). The corrected vibrational populations for the $v''=0$ and $v''=1$ levels yield a ratio of 4.1×10^{-4}.

Within the limits of experimental error the population ratio $CH(v=0)$ to $CH(v=1)$ is indifferent to vibrational excitation of H_2. Difference measurements with our trigger suspending device yielded no changes: neither the total population of the $v''=1$ state nor the population of single rotational states increased. From the S/N ratio of the spectra and the spectral line intensities we estimate that intensity differences between the $H_2(v=0)$ and $H_2(v=1)$ reaction have to be smaller than 20% for $CH(v''=1)$, if they should occur.

Rotational distribution

The population of the rotational energy states of the CH product in $v''=0$ can be approximately described by the Boltzmann distribution law. This does not hold for the higher rotational states, $N''=12$ to 14. Omitting the lines up to $N''=3$, which underwent relaxation, we found rotational temperatures of (1930 ± 190) K for the Q and (1230 ± 100) K for the P branch. This is in fairly good agreement with Ref. 11, although they found a slightly higher temperature for the P branch ($T=1580$ K).

For the vibrationally excited state of CH the rotational state population can also be described by a Boltzmann distribution, but the temperature parameter is 340 K.

The influence of H_2 vibrational excitation on the rotational distribution of $CH(v''=0)$ was determined more distinctly than it was possible for the vibrational distribution of CH. The reaction of $C(^1D)$ with $H_2(v=1)$ results

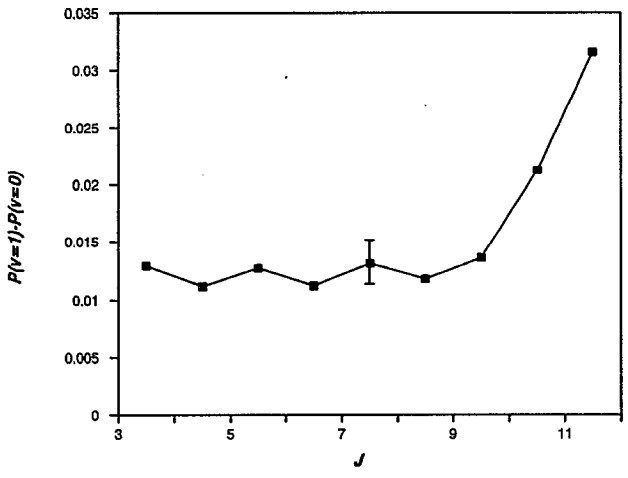

FIG. 3. Plot of the relative population differences in the respective rotational states as measured with and without vibrationally excited hydrogen. A positive sign indicates an increase in population when $H_2(v=1)$ is present.

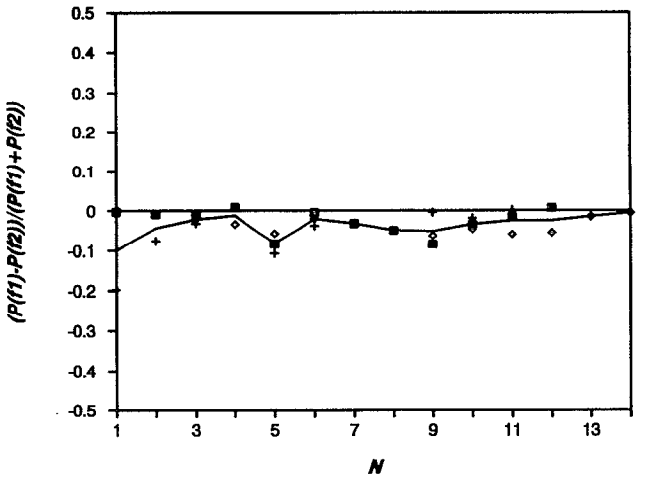

FIG. 4. Normalized population ratio of the spin–orbit states of CH where the degeneracy has been taken into account. The solid line is the average of +: R branches; ●: P branches; □: Q branches.

in a population enhancement of the rotational states of CH, as shown in Fig. 3. With respect to the populations in the lower rotational states, the population in $N''=12$ increases by 2%. The values in Fig. 3 are the result of a difference measurement of LIF intensities with and without excitation of H_2. The error of every single population difference measurement has been extracted from the S/N ratio and is less than 10% due to averaging over 100 laser shots per recording channel. The signal increase indicates an enhancement of the reaction rate constant for $H_2(v=1)$ compared to $H_2(v=0)$.

Electronic fine structure distribution

Two types of electronic fine structure have to be considered here, the spin–orbit and the Λ splitting. The former originates from interaction of the orbital angular momentum with the spin of the unpaired electron, the latter from interaction of the angular momentum with the nuclear rotation. In Fig. 4 the relative spin–orbit state population differences, $[P(f_1)-P(f_2)]/[P(f_1)+P(f_2)]$, are plotted against J, where the different degeneracies of the states are taken into account. f_1 and f_2 denote the spin substates of the electronic ground state, F_1 and F_2 denote the spin substates of the electronically excited state. There is a very weak preponderance for the f_2 spin system when the populations of the f_1 spin–orbit component ($J=N+1/2$) is compared with the f_2 component of CH($J=N-1/2$). This is due to energetic reasons because the respective level in f_2 has a lower energy than the one in the f_1 system. There is no deviation from this rule in the CH spectra, nor is there any J dependence observable.

The population of the Λ states appears to be different. In Fig. 5 the normalized population difference of the antisymmetric $\Pi(A'')$ states and the symmetric $\Pi(A')$ states is plotted. The symmetry plane is the plane of rotation which corresponds to the plane of the reaction if the geometry remains planar. $\Pi(A'')$ states are probed by P, R lines and $\Pi(A')$ states by Q lines.[24(b)] As can be seen, the plot of

$$f_\Lambda=\frac{P[\Pi(A'')]-P[\Pi(A')]}{P[\Pi(A'')]+P[\Pi(A')]} \tag{4}$$

vs J shows negative values, indicating a higher propensity for the generation of CH molecules in the symmetric $\Pi(A')$ state.

The Λ selectivity is influenced by the use of vibrationally excited hydrogen in the reaction. In this case the selectivity decreases, i.e., the population of the $\Pi(A')$ levels decreases (Fig. 5). This change to a more statistical distribution of the molecules among their Λ substates allows

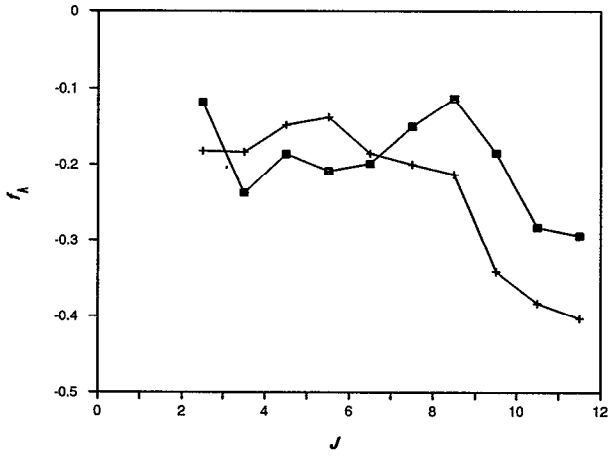

FIG. 5. Normalized population ratio f_Λ of the Λ substates of CH. The squares represent the reaction with $H_2(v=1)$, the crosses the reaction with $H_2(v=0)$. A considerable difference appears for the high-J limit ($J>6$) where the population of the Λ substates can be related to the geometry of the collision process.

important insights into the mechanism of the reaction. This will be discussed in more detail in the next main section.

Influences from further reactions

The reaction of ground state carbon atoms

$$C(^3P)+H_2 \xrightarrow{M} CH+H \tag{5}$$

at room temperature is a slow third order process with a rate constant of about 7×10^{-32} $cm^6\,molecule^{-2}\,s^{-1}$ (Refs. 26–29) for M=He. The reaction energy is $\Delta H_r^0(0\ K)=97.3\ kJ\ mol^{-1}$, thus the reaction is strongly endothermic. Nevertheless, this reaction reaches considerable velocities at high temperatures. Dean *et al.*[30] have measured a temperature dependent second order rate constant of

$$k=6.64\times10^{-10}\exp[-11\,700\ K/T]\,cm^3\,molecule^{-1}\,s^{-1} \tag{6}$$

between 1525 and 2540 K. The photolysis of carbon suboxide at 157 nm yields 97% $C(^3P)$ and 3% $C(^1D)$, the former with a kinetic energy corresponding to a temperature of 3040 K.[17] The center-of-mass kinetic energy, $E_{c.m.}(C,H_2)$ in the collision system $H_2+C(^3P)$ is calculated by

$$E_{c.m.}(C,H_2)=\tfrac{1}{2}\mu(C,H_2)\cdot[\langle v_{H_2}^2\rangle+\langle v_C^2\rangle+\langle v_{C_3O_2}^2\rangle]. \tag{7}$$

$\sqrt{\langle v_C^2\rangle}$ has been measured directly[17] to be 2540 ms^{-1}, $\langle v_{H_2}^2\rangle$ and $\langle v_{C_3O_2}^2\rangle$ are in a thermal equilibrium at room temperature, thus the equation

$$\langle v^2\rangle=\frac{3\,RT}{m} \tag{8}$$

is applicable. This results in $E_{c.m.}=8.67\ kJ\ mol^{-1}$ and from $E_{c.m.}=3/2\ RT$ an averaged "collisional temperature" of 700 K can be obtained. This is outside of the temperature range for which Eq. (6) was obtained, but for a rough estimate this results in $k=3.3\times10^{-17}\ cm^3\ molecule^{-1}\ s^{-1}$. Under our experimental conditions, the ratio of the yields of the respective reactions is

$$f[C(^1D)]\approx\frac{k(C(^1D)]}{k[C(^3P)]}\cdot\frac{\phi[C(^1D)]}{\phi[C(^3P)]}\approx3.8\times10^4 \tag{9}$$

when $\phi[C(^1D)]=0.03$, $\phi[C(^3P)]=0.97$, and $k[C(^1D)]=4.1\times10^{-11}\ cm^3\ molecule^{-1}\ s^{-1}$ [the smallest rate constant reported yet[6]] is used. Thus we do not expect any observable influence from the reaction of ground state carbon.

Apart from reactions (3) and (5) there are further processes within the C_3O_2/H_2 system that should be discussed. Electronically excited carbon atoms are removed by carbon suboxide

$$C(^1D)+C_3O_2\rightarrow P. \tag{10}$$

This reaction has not been described in the literature. We expect it to happen because $C(^3P)$ and $C(^1S)$ react with C_3O_2 at rate constants of $1.8\times10^{-10}\ cm^3\ molecule^{-1}\ s^{-1}$ for $C(^3P)$ (Ref. 26) and $1\times10^{-10}\ cm^3\ molecule^{-1}\ s^{-1}$ for $C(^1S)$.[31] These are rates for the removal of atomic carbon, without characterization of the products. Reaction (10) does not lead to an altered CH product state distribution, because it just removes $C(^1D)$ from the reaction zone, i.e., it decreases the signal intensity but does not disturb the measurements. Only products of this reaction (10) might interfere in secondary reactions with the CH of reaction (3).

Umemoto *et al.*[32] observed emission from electronically excited C_2 in the 193 nm laser photolysis of C_3O_2. The production of $C_2(d\,^3\Pi_g)$ is ascribed to the reaction of $C(^3P)$ with $C_2O(\tilde{a}\,^1\Delta)$, the latter probably being generated in the 157 nm photolysis also.[17] We are unaware of a reaction rate for

$$C_2(d\,^3\Pi_g)+H_2\rightarrow CH+CH, \tag{11}$$

but this reaction is endothermic by about 120 $kJ\ mol^{-1}$ and not likely to produce large amounts of CH, because C_2 has to be produced first. The evolution time of the C_2 emission is roughly 400 ns,[32] and the subsequent reaction with H_2 might be slow, since the reaction of ground state C_2 with H_2 has a reaction rate of 3×10^{-14} $cm^3\ molecule^{-1}\ s^{-1}$.[33]

A reaction of hydrogen with C_2O in the ground state

$$C_2O(\tilde{X}\,^3\Sigma^-)+H_2\rightarrow P \tag{12}$$

has been observed at a rate constant of 2×10^{-14} $cm^3\ molecule^{-1}\ s^{-1}$.[34] Therefore, this reaction will not influence the observed CH product state distribution. Reactions of hydrogen atoms have not been considered because H is only a product of reaction (3) and thus the generation of any products is slower than (3).

DISCUSSION

The available energy E_{av}, which is partitioned among the degrees of freedom of the reaction products H and CH, is given by

$$E_{av}=\Delta H^0+E_{int}(H_2)+E_{c.m.}(C,H_2). \tag{13}$$

$E_{int}(H_2)$ is the rotational energy of molecular hydrogen at room temperature. It is calculated from the Boltzmann distribution law to be 190 cm^{-1} under consideration of the statistical weights of the nuclear spin states. The center-of-mass energy of the C, H_2 system, $E_{c.m.}(C,H_2)$, can be calculated from Eq. (7). With a rms speed of 1520 ms^{-1} for the $C(^1D)$ atoms[17] an average kinetic energy of 440 cm^{-1} is obtained. The reaction enthalpy $\Delta H_r^0(0\ K)$ equals 2040 cm^{-1},[35] so the available energy for the H and CH products is 2670 cm^{-1}, which is an average energy due to the thermal distribution of the reactants.

The available energy E_{av} has a different value for reactions with vibrationally excited H_2. In that case the energy of the vibrational quantum of H_2 has to be added to $E_{int}(H_2)$, and one obtains $E_{int}(H_2)\approx190\ cm^{-1}+4155\ cm^{-1}=4345\ cm^{-1}$ and $E_{av}=6825\ cm^{-1}$.

TABLE I. Partition of the energy (cm^{-1}) into vibrational, rotational, and translational motion of the CH product.

	E_{av}	E_{vib}	E_{rot}	E_{trans}	f_{vib}	f_{rot}	f_{trans}
$H_2(v=0)$	2670	1.1	707	1960	4.1×10^{-4}	0.26	0.74
$H_2(v=1)$	6825	1.1	1237	5585	1.6×10^{-4}	0.18	0.82

The Boltzmann plot of the CH rotational distribution did not show exact linearity, so the rotational energy was calculated according to

$$E_{rot}=\sum_J P(J)\cdot E(J), \tag{14}$$

where $P(J)$ is the normalized CH rotational state distribution and $E(J)$ is the energy of the rotational state J.

For the reaction with $H_2(v=0)$ this results in $E_{rot}=707\ cm^{-1}$, for the $H(v=1)$ case a value of $E_{rot}=813\ cm^{-1}$ is measured. The increase of 106 cm^{-1} is caused by the fraction of 20% of H_2 that has been excited to $v=1$. Thus the rotational energy increases from 707 to 1237 cm^{-1} for the case of pure vibrationally excited H_2 as reaction partner of C(^1D). In the following we shall always refer to pure $H_2(v=1)$.

The calculation of the CH vibrational energy content yields

$$E_{vib}=\omega_0(v=1)\cdot P(v=1)$$
$$=2733\ cm^{-1}\cdot 4.1\times10^{-4}=1.1\ cm^{-1}.$$

when the ground state term value $\omega_0(v=1)=2733\ cm^{-1}$ is taken.[20,21] Even if there were an increase in the population of the $v''=1$ state of 20%, which is within the experimental uncertainty determined from the S/N ratio, it would not alter the contribution of the vibrational energy to the total energy release significantly because of the negligible amount of E_{vib}.

The translational energy E_{trans} is obtained as the difference between E_{av} and the sum of E_{rot} and E_{vib} due to conservation of energy. The respective values for the translational energies and the partition numbers, $f_{rot}=E_{rot}/E_{av}$ and $f_{trans}=E_{trans}/E_{av}$, are summarized in Table I.

The predicted CH($v=0$) rotational distribution derived from classical trajectory studies differs from the one that has been observed experimentally. However, the prior distribution $P^0(v=0,J)$ based on a completely statistical partitioning of energy into the fragments[36] fits the experimental distribution very well, as was already shown by Jursich and Wiesenfeld for CH($v=0$).[9] Therefore, it is useful to compare the experimental observations with the prior distribution $P^0(v=1,J)$ for CH($v=1$) and the ratio $P^0(v=1)/P^0(v=0)$ of the vibrational state populations.

Since the formation of CH in the first vibrational excited state is an endothermic process, it is obligatory to account more realistically for the thermal reagent energy than in Eq. (13) where only average values were used. This was performed by numerical integrating over the translational energy contribution to the available energy E_{av}

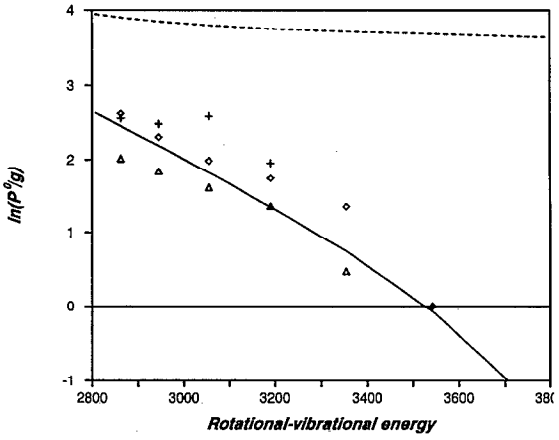

FIG. 6. Population of CH rotational states in the vibrationally excited state $v=1$. +:Q, ●:P, □:R branches. The solid line represents a thermally averaged prior distribution when H_2 ($v=0$) is used as reactant. The dashed line shows the corresponding prior calculation with the vibrationally excited reagent, $H_2(v=1)$.

$$P^0(v,J)\sim(2J+1)\int[E_{av}-E(v,J)]^{1/2}f(v)dv \tag{15}$$

with

$$E_{av}=E_0+\frac{\mu(C,H_2)}{2}v^2. \tag{16}$$

E_0 contains all energies which are independent of the collisional velocity. $f(v)$ is the Maxwell–Boltzmann velocity distribution function where the C(^1D) velocity distribution is considered. The solid line in Fig. 6 represents the obtained prior distribution ($P^0(v=1,J)$ which fits the observed rotational distribution of CH in $v=1$ very well. This implies that the available energy is distributed statistically among the rotational states of the CH product when $H_2(v=0)$ is used as a reactant.

For a statistical product energy distribution the lifetime of the collision complex has to be long enough (at least several vibrational periods) to allow internal energy randomization prior to dissociation into the CH(J) and H fragments. This is supported by a RRKM calculation of the lifetime of an assumed $CH_2(\tilde{a}\,^1A_1)$ collision complex which yields a value of about 1 ps.[9] Furthermore, the exit channel of the reaction complex should be smooth, because any strong anisotropic forces would transfer the energy nonstatistically to the rotational states of the CH products. The macroscopic branching ratio between CH and CD in the reaction of C(^1D) and HD also supports the model of a statistical energy distribution. Fisher *et al.* showed that their observed branching ratio of [CD]/[CH]=1.69 is comparable to the result of a simple RRK calculation based on a collision complex with insertion of the carbon atom into the HD bond yielding a branching ratio of [CD]/[CH]=1.7.

The results from an analogous calculation for the reaction of $H_2(v=1)$ are different. In this case the theoretically obtained prior distribution is much broader than for $H_2(v=0)$ as is indicated by the dashed line in Fig. 6, what contrasts our experimental observation that the rotational state population of vibrationally excited CH remains unaltered when $H_2(v=1)$ is present. Therefore, we conclude that the simple statistical model is not valid for the $H_2(v=1)$ reaction, and mode specific reaction paths become important. The lifetime of the collision complex should be reduced strongly.

The prior distribution $P^0(v)$ of the vibrational states is given by a summation over J up to the highest accessible state, $P^0(v)=\Sigma\, P^0(v,J)$. In the case of $H_2(v=0)$ a theoretical population ratio of $P^0(v=1)/P^0(v=0)=1.8\times10^{-2}$ is obtained, which is significantly higher than the experimentally observed value of $P_{exp}(v=1)/P_{exp}(v=0)=4.1\times10^{-4}$. Thus the randomization of the available energy does not involve all degrees of freedom. The transfer of translational motion of the reactants to product vibration is less effective than expected from simple energy considerations and the CH vibrational distribution is controlled rather dynamically than statistically.

The deviation from a statistical distribution is much more evident when vibrationally excited H_2 is used as a reactant. In this case one expects a prior population ratio of $P^0(v=1)/P^0(v=0)=0.48$ which is more than three orders of magnitude higher than the observed value for $H_2(v=1)$. Again, it seems to be likely that mode specific reaction paths become important. It should be remembered, however, that $H_2(v=1)$ as reactant does influence the reaction dynamics (Figs. 3 and 5, Table I), but in a different way than expected on simple statistical grounds.

Questions related to the reaction geometry are most decisively answered by examining the Λ-state distribution, which reflects the symmetry conservation in dissociative and reactive processes. Reactants which are symmetric (antisymmetric) with respect to the point group of the collision geometry will be transformed to products which are also symmetric (antisymmetric). For a planar reaction geometry, where the $C(^1D)$ inserts in the H_2 bond (C_{2v} symmetry), the transition state is described by the $CH_2(\tilde{a}\,^1A_1)$ electronic state. In the course of this insertion reaction the highly excited $CH_2(\tilde{a}\,^1A_1)$ dissociates into the products CH and H. Since the $^1A_1$ state is symmetric with respect to the plane of the reaction, the products have to be symmetric with respect to this plane as well. The hydrogen atom is formed in the symmetric ^2S state; therefore one expects CH products to be formed in the symmetric $\Pi(A')$ state. This is only valid in the high-J limit where the symmetry $\Pi(A')$ and $\Pi(A'')$ is well defined. Due to the small ratio $A/B=2.0$ of the spin–orbit coupling constant A to the rotational constant B the CH molecule reaches the theoretical maximum degree of electronic alignment[37] already at $N''=6$, in contrast, e.g., to OH where the corresponding rotational level is $N''=15$.

Comparable to reaction (2) we found a higher propensity for the generation of CH molecules in the molecular state $\Pi(A')$ which is symmetric with respect to the plane in which the reactive collision between $C(^1D)$ and H_2 occurs. This behavior also holds for the reaction of vibrationally excited hydrogen, but in the high-J limit the selectivity decreases from $f_\Lambda=0.25$ for $H_2(v=0)$ to $f_\Lambda=0.15$ for $H_2(v=1)$. At first we want to consider the consequence of an insertion mechanism for the reaction. When the C atom inserts into the H_2 bond and reaches the well on the $CH_2(\tilde{a}\,^1A_1)$ surface one can regard this transition state as a highly excited bending mode of CH_2 in the first singlet state. A transfer of energy from this bending motion to the asymmetrical stretch leads to rotating CH products. A similar picture is revealed for the reaction of $O(^1D)$ with H_2. However, in that case a higher OH rotation and a much stronger pronounced Λ-state selectivity are observed. The weakly pronounced Λ-state selectivity implies that the $C(^1D)+H_2$ collision complex lives long enough so that out-of-plane motions during the reactive encounter become important, i.e., the duration of the reaction should be on the order of a rotational period of $CH_2(\tau_D\approx0.5$ ps).

The alternative mechanism is the abstraction reaction that proceeds via a linear H–H–C collision complex with $C_{\infty v}$ elements of symmetry. In this case no selectivity regarding CH in the $\Pi(A')$ or $\Pi(A'')$ states is expected and a statistical population with respect to these states will result. However, the abstraction reaction will not be the major reaction path, because the $C_{\infty v}$ surface exhibits a late barrier hindering the collision complex from dissociating into CH+H, in contrast to the C_{2v} potential energy surface which does not show any barrier and consists of the deep well at the $CH_2(\tilde{a}\,^1A_1)$ equilibrium configuration. Different values for the barrier height on the $C_{\infty v}$ surface have been calculated lying in the range of 40.5 kJ mol^{-1} (Ref. 14) to 62.7 kJ mol^{-1}.[12] Despite this uncertainty it is clear that the insertion mechanism dominates the abstractive mechanism because the height of the barrier is well above the available energy $E_{av}=31.9$ kJ mol^{-1} for $H_2(v=0)$. The trajectory calculations by Whitlock *et al.*[12] resulted in an insertion path for more than 99% of the total amount of trajectories.

The existence of a late barrier for the abstraction path allows the prediction that vibrational excitation of the H_2 reactant accelerates the reaction, i.e., increases the probability for the abstraction reaction. An increase in the reaction rate is observed in the present experiment when vibrationally excited H_2 is used. The Λ selectivity of the CH generation decreases when vibrationally excited H_2 takes part in the reaction, f_Λ increases from -0.25 to -0.17 for this case.

It is also possible that the higher amount of available energy in the case of $H_2(v=1)$ will lead to a highly excited transition state of the $CH_2(\tilde{a}\,^1A_1)$ collision complex which dissociates much faster than in the $H_2(v=0)$ case. For a fast dissociation less time is left for an energy randomization and the products should be formed with a nonstatistical distribution. Although this is observed in the experiment (see Table I) it is expected that the symmetry of a prompter reaction should be conserved to a greater extent, and a much stronger Λ selectivity [similar to the $O(^1D)+H_2$ reaction] would be predicted. Since the population of

the Λ states is less specific with $H_2(v=1)$ as reactant it seems to be more likely that the abstraction channel becomes important. With $H_2(v=1)$ there is not only sufficient energy available to pass the barrier, but also the motion of the nuclei is in the direction of the reaction path.

In summary, vibrational excitation of H_2 increases the reaction rate and the CH rotational energy. However, the CH rotational excitation becomes lower than expected from statistical considerations. The CH vibrational excitation remains low, independent of the vibrational excitation of the H_2 reactant. The translational motion of the reactant is inefficiently transferred to CH vibrational motion. The reaction is dominated by an insertion process when $H_2(v=0)$ as reactant is used. For vibrationally excited H_2 our observations indicate a change of the reaction geometry and an abstraction process seems to become important.

ACKNOWLEDGMENTS

We thank Professor Dr. F. J. Comes for helpful discussions and material support. This work was performed as part of a programme of the Deutsche Forschungsgemeinschaft (DFG).

[1] C. Hsiao, A. Sinha, and F. F. Crim, J. Phys. Chem. **95**, 8263 (1991).
[2] M. Meier, G. Ahlers, and H. Zacharias, J. Chem. Phys. **85**, 2599 (1986).
[3] Y. Zhu, Y. Huang, S. Arepalli, and R. J. Gordon, J. Appl. Phys. **67**, 604 (1990).
[4] (a) D. A. V. Kliner and R. N. Zare, J. Chem. Phys. **92**, 2107 (1990). (b) D. Neuhauser, R. S. Judson, D. J. Kouri, D. E. Adelman, N. E. Shafer, D. A. V. Kliner, and R. N. Zare, Science **257**, 519 (1992).
[5] K. Mikulecky and K.-H. Gericke, J. Chem. Phys. **96**, 7490 (1992).
[6] W. Braun, A. M. Bass, D. D. Davis, and J. D. Simmons, Proc. R. Soc. London, Ser. A **312**, 417 (1969).
[7] D. Husain and L. J. Kirsch, Chem. Phys. Lett. **9**, 412 (1971).
[8] K. Schofield, J. Phys. Chem. Ref. Data **8**, 723 (1979).
[9] G. M. Jursich and J. R. Wiesenfeld, Chem. Phys. Lett. **110**, 14 (1984).
[10] G. M. Jursich and J. R. Wiesenfeld, J. Chem. Phys. **83**, 910 (1985).
[11] W. H. Fisher, T. Carrington, and C. M. Sadowski, Chem. Phys. **97**, 433 (1985).
[12] P. A. Whitlock, J. T. Muckerman, and P. M. Kroger, in *Potential Energy Surfaces and Dynamics Calculations*, edited by D. G. Truhlar (Plenum, New York, 1981).
[13] R. J. Blint and M. D. Newton, Chem. Phys. Lett. **32**, 178 (1975).
[14] S. A. Alexander, C. McDonald, and F. A. Matsen, Int. J. Quantum Chem. Quantum Chem. Symp. **17**, 407 (1983).
[15] R. Schinke, W. A. Lester, J. Chem. Phys. **72**, 3754 (1980).
[16] (a) P. A. Berg, J. J. Sloan, and P. J. Kuntz, J. Chem. Phys. **95**, 8038 (1991); (b) *ibid.* **96**, 6324 (1992).
[17] C. E. M. Strauss, S. H. Kable, G. K. Chawla, P. L. Houston, and I. R. Burak, J. Chem. Phys. **94**, 1837 (1991).
[18] S. V. Filseth, Adv. Photochem. **10**, 1 (1977).
[19] O. Diels and G. Meyerheim, Ber. Dtsch. Chem. Ges. **40**, 355 (1907).
[20] G. Herzberg and J. W. C. Johns, Astrophys. J. **158**, 399 (1969).
[21] P. F. Bernath, C. R. Brazier, T. Olsen, R. Hailey, W. T. M. L. Fernando, C. Woods, and J. L. Hardwick, J. Mol. Spectrosc. **147**, 16 (1991).
[22] L. Gerö, Z. Phys. **118**, 27 (1941).
[23] S. V. Filseth, H. Zacharias, J. Danon, R. Wallenstein, and K. H. Welge, Chem. Phys. Lett. **58**, 140 (1978).
[24] (a) P. A. Bonczyk and J. A. Shirley, Combust. Flame **34**, 253 (1979); (b) M. H. Alexander, P. Andresen, R. Bacis, R. Bersohn, F. J. Comes *et al.*, J. Chem. Phys. **89**, 1749 (1988).
[25] Spectroscopic Data, Vol. 1A, edited by S. N. Suchard (IFI/Plenum Data, New York, 1975).
[26] D. Husain and A. N. Young, J. Chem. Soc. Faraday Trans. 2 **71**, 525 (1975).
[27] D. Husain and L. J. Kirsch, Chem. Phys. Lett. **8**, 543 (1971).
[28] D. Husain and L. J. Kirsch, Trans. Faraday Soc. **67**, 2025 (1971).
[29] F. F. Martinotti, M. J. Welch, and A. P. Wolf, Chem. Commun. **1968**, 15.
[30] A. J. Dean, D. F. Davidson, and R. K. Hanson, J. Phys. Chem. **95**, 183 (1991).
[31] D. Husain and L. J. Kirsch, J. Photochem. **2**, 297 (1974).
[32] M. Umemoto, H. Shinohara, N. Nishi, and R. Shimada, J. Photochem. **20**, 277 (1982).
[33] H. Reisler, M. S. Mangir, and C. Wittig, J. Chem. Phys. **73**, 2280 (1980).
[34] V. M. Donnelly, W. M. Pitts, and J. R. McDonald, Chem. Phys. **49**, 289 (1989).
[35] D. L. Baulch, R. A. Cox, R. F. Hampson, J. A. Kerr, J. Troe *et al.* J. Phys. Chem. Ref. Data **13**, 1259 (1984).
[36] R. D. Levine and R. B. Bernstein, *Molecular Reaction Dynamics and Chemical Reactivity* (Oxford University, Oxford, 1987).
[37] L. Bigio and E. R. Grant, J. Chem. Phys. **87**, 5589 (1987).